Electronic Supplementary Material (ESI) for Journal of Materials Chemistry A.

Interweaving 3D ion-conductive network binder for high-loading and lean-electrolyte lithium-sulfur batteries

Jing Chen,[a] Xin Geng,[a] Chenyang Wang,[a] Xu Hou,[b] Hailong Wang,[a] Qinlang Rong,[a] Nuo Sun,[a] Wei Liu,[a] Linyu Hu,[c] Xiaowei Fu,[d] Jingxin Lei,[d] Zhimeng Liu*[a] and Xin He*[a]

[a] School of Chemical Engineering, Sichuan University, Chengdu, 610065, China

[b] Department of Chemistry-Ångström Laboratory, Uppsala University, Regementsvägen, 175237, Uppsala, Sweden

[c] School of Microelectronics, Southern University of Science and Technology, Shenzhen, 518055, China

[d] State Key Laboratory of Polymer Materials Engineering, Polymer Research Institute, Sichuan University, Chengdu, 610065, China

* Corresponding author

E-mail addresses: zhimengliu@scu.edu.cn; xinhe@scu.edu.cn

1. Materials and methods

1.1. Materials

Polyethylene glycol (PEG, Mw=~4000), triethylamine (TEA), ethylenediamine (EDA), carbon disulfide (CS_2), isopropanol (IPA) and N,N-Dimethylformamide (DMF) were purchased from Chengdu Kelong Chemical Reagent Co. Ltd (Chengdu, China). Polyethylene oxide (PEO, Mw=~600000), dimethylolpropionic acid (DMPA), isophorone diisicyanate (IPDI), and dibutyltin dilaurate (DBTDL) were purchased from Shanghai Titan Scientific Co. Ltd. (Shanghai, China). Trimethylolpropane polyethylene glycol monomethyl ether (Ymer N120, reagent grade, Mw=~1000) was obtained from Perstorp in Sweden. Poly (vinylidene fluoride) (PVDF, Mw=~534000), sulfur (S_8 sublimed powder, reagent grade), and lithium nitrate (99.9%) were purchased from Aladdin. Multi-walled carbon nanotube (MWCNT, 99%) was obtained from Shenzhen Huiheng Scientific Co. Ltd. Super P was provided by Neware Technology Co. Ltd (Shenzhen, China). 1,3-dioxolane (DOL, anhydrous), 1,2-dimethoxyethane (DME, anhydrous), and LS001 electrolyte were provided by DodoChem. Trimethylolpropane tris(2-methyl-1-aziridinepropionate) (HD-100A) was obtained from Ningxia Zhuoyu New Materials Co. Ltd (Ningxia, China). Before use, PEG, Ymer N120, and DMPA were dried under a vacuum condition at 105 °C for 2 h.

1.2. Experimental section

1.2.1 The preparation of waterborne polyurethane (WPU) solution

The preparation route of the WPU solution is shown in Fig. S1, and the molar quantities of used materials are listed in Table S1. Firstly, the PEG, Ymer N120, DMPA, IPDI, and a catalytic amount of DBTDL were added into a 250 ml three-round bottom flask with an overhead stirrer and reacted at 85 °C for 7 h to obtain prepolymer. Secondly, the prepolymer was cooled to 50 °C, and the TEA was added. Afterward, the deionized water was gradually introduced into the prepolymer under stirring to obtain the waterborne prepolymer dispersion. Finally, an EDA aqueous solution (where ethylenediamine was dissolved in deionized water) was dropped into the dispersion under continuous agitation for 30 minutes to complete the chain

extension at 25 °C. The high molecular WPU emulsion was obtained after 1 h of stirring.

1.2.2 Electrode preparation and battery fabrication

The Carbon-Sulfur (C/S) composite was prepared according to the published literature,[1] by wetting MWCNTs with a sulfur solution (CS_2/IPA) in a Teflon vessel. The mixture was then dried at 45 °C (MWCNTs: sulfur=3:7) for 12 h and subsequently further dried at 60 °C for 3 h in a vacuum oven to obtain a C/S composite. To prepare the sulfur electrode, the homogeneous slurry was prepared by mixing the C/S composite, Super P, graphene, WPU, and HD-100A (C/S composite: Super P: graphene: CWPU=8:0.5:0.5:1) under ball-milling. Subsequently, the slurry was coated on the current collector with a doctor-blade coating method, and the electrode was dried at 50 °C for 1 h. The resulting electrode was then cut into smaller units with an area of 1.13 cm^2 and further dried in a vacuum oven at 50 °C for 24 h. For comparison, sulfur electrodes using PVDF and PEO as binders were prepared in the same processes, distilled water was used as dispersant for PEO, and NMP for PVDF.

The prepared electrode was assembled CR2032 coin-type half-cells in an Ar-filled glove box by sandwiching the separator (Celgard 2400) between the prepared electrode and metallic lithium wafer. 1.0 M LiTFSI in 1:1 DOL/DME containing 1 wt% $LiNO_3$ was used as the electrolyte.

1.3. Characterization

1.3.1 Electrochemical measurements

Discharge and charge tests were conducted using a MIHW-200-160CH constant temperature test box (Shenzhen Neware Technology Co. Ltd) at 30 °C within the voltage range of 1.7-2.8 V. Cyclic voltammetry (CV) tests of the electrodes were conducted in the potential range of 1.7-2.8 V with a scan rate of 0.033 mV s^{-1}, and electrochemical impedance spectroscopy (EIS) tests were performed over a frequency range of 10^5 Hz to 0.01 Hz, both on the Metrohm VIONIC electrochemical workstation.

1.3.2 Ionic conductivity test

The Lithium-ion conductivity of different binder membranes was measured by electrochemical impedance spectroscopy (EIS) using a Metrohm VIONIC electrochemical workstation. Typically, a CWPU film with a small amount of LiTFSI (with a mass ratio of LiTFSI to polymer of 1:2) was sandwiched between two stainless-steel electrodes and then assembled into a CR2032 coin cell. The EIS of the sample was measured in the frequency range from 10^7 Hz to 0.1 Hz at 30 °C. Other membranes were also conducted through the same measurement procedures. The Li-ion conductivity of different binders can be calculated by the following equation:

$$\sigma = \frac{L}{A \times R}$$

Where L is the distance between the two electrodes, A is the contact area of two electrodes, and R is the impedance of binder films with LiTFSI.[2]

1.3.3 Materials characterization

The particle size of WPU solution was measured with a nanoparticle size analyzer (Zetasizer Nano ZS90). FTIR was employed on an infrared spectrometer (Nicolet iS50, America) to study the chemical structure of WPU and CWPU film. ^{1}H NMR was performed on NMR spectrometer (JNM-ECZ400S/L1) at 400MHz with the DMSO-d6 as solvent to confirm the structure of WPU. INS Tron Universal Material Testing Machine (5967, America) was used for tensile test to measure the mechanical properties of different binders. DSC (Q250, American) was used to detect the thermal transition behaviors of CWPU and CWPU-WY between -70 °C to 80 °C at a rate of 10 °C min^{-1}. The thermal stability of the CWPU binder was detected by heating from room temperature to 600 °C with a thermogravimetric analysis (TGA, SDTQ600, America). The contact angle of electrodes with different binders were measured with a contact angle measurement (DSA30S) to confirm the electrolyte wettability of CWPU, PEO, and PVDF binders. XPS measurements on lithium anode and films of different binders were conducted with an AXIS Supra+ (Kratos with a focused 20-500 μm diameter beam of monochromatic X-rays and a 15 kV filament voltage source energy). The Al Kα radiation with an energy of 1486.3 eV and an angle of 0° of emission was used for the measurements. Sputtering was performed

using a monoatomic Ar+ source operated at 5 keV. The SEM (JSM 7610F) was used for observing the morphologies of cathodes and anodes. In-situ Raman was performed on a DXR Raman Microscope (Thermo Fisher Scientific) with a 455 nm laser to observe the shuttle effect of Li-S batteries.

1.3.4 Peel test

A rectangular sulfur cathode sheet with a length of 5 cm and a width of 2.4 cm was fixed on a glass slide, and the active material side was adhered to the 3M tape. The peel strength of the cathodes was measured by a tensile machine (INS Tron Universal Material Testing Machine, 5967, America) at a stretching speed of 10 mm min^{-1} with 180°.

1.3.5 In-situ UV-visible spectroscopy (UV-vis) spectroscopy test

The Li_2S and S were uniformly mixed in the electrolyte (1.0 M LiTFSI in 1:1(v/v) DOL/DME containing 1 wt% $LiNO_3$) with a molar ratio of 1:5 to form a 0.25 M Li_2S_6 solution. The mixing process was carried out with magnetic stirring in an Ar-filled glove box. Nickel foam loaded with CWPU, PEO, and PVDF binders in equal amounts was added to the solution containing 5 μL prepared Li_2S_6 solution in 2 mL of electrolyte. In-situ UV-visible spectroscopy (UV-vis, UV1500PC) was employed to detect adsorption signal of Li_2S_6 during 12 h.

1.3.6 Li_2S nucleation

Li_2S and S were uniformly mixed in the electrolyte of Li-S batteries (1.0 M LiTFSI in 1:1(v/v) DOL/DME containing 1 wt% $LiNO_3$) with a ratio of 1:7, and stirred at the Ar-filled atmosphere to prepare a 0.5 M Li_2S_8 solution. The carbon paper was loaded with equal amounts of CWPU, PEO, and PVDF binders (CWPU@CP, PEO@CP, and PVDF@CP) and dried overnight. In an Ar-filled glove box, 20 μL of Li_2S_8 solution was dropped onto the CWPU@CP, PEO@CP, and PVDF@CP as cathodes, and 20 μL of Li-S electrolyte was added to assemble the batteries. After a continuous discharge with a constant current of 0.112 mA to 2.15 V,

potentiostatically discharged at 2.1 V until the current diminishes to a level below 0.01 mA.

1.3.7 Density Functional Theory (DFT) calculation method

The binding energy between different binders and LiPSs was calculated with Materials Studio based on the first-principal method. The generalized gradient approximation (GGA) and the Perdew-Burke-Ernzerhof (PBE) function were used to calculate electron exchange and correlation.[3] The electronic calculation uses a double numerical orbital basis set orbital polarization function (DNP). The SCF generation error and K point are set to 1.0×10^{-6} Ha and 3x3x1, respectively. The vdW-DF2 correction used in the calculation uses the TS method.

The adsorption energy between different binders and LiPSs was calculated with the following formula:

$$\Delta E_{LiPSs} = E_{binder+LiPSs} - E_{binder} - E_{LiPSs}$$ [4]

where $E_{binder+LiPSs}$, E_{binder}, and E_{LiPSs} are the energies of the total energy of binder-LiPSs complex, different binders, and lithium polysulfides.

2. Supplementary Figure

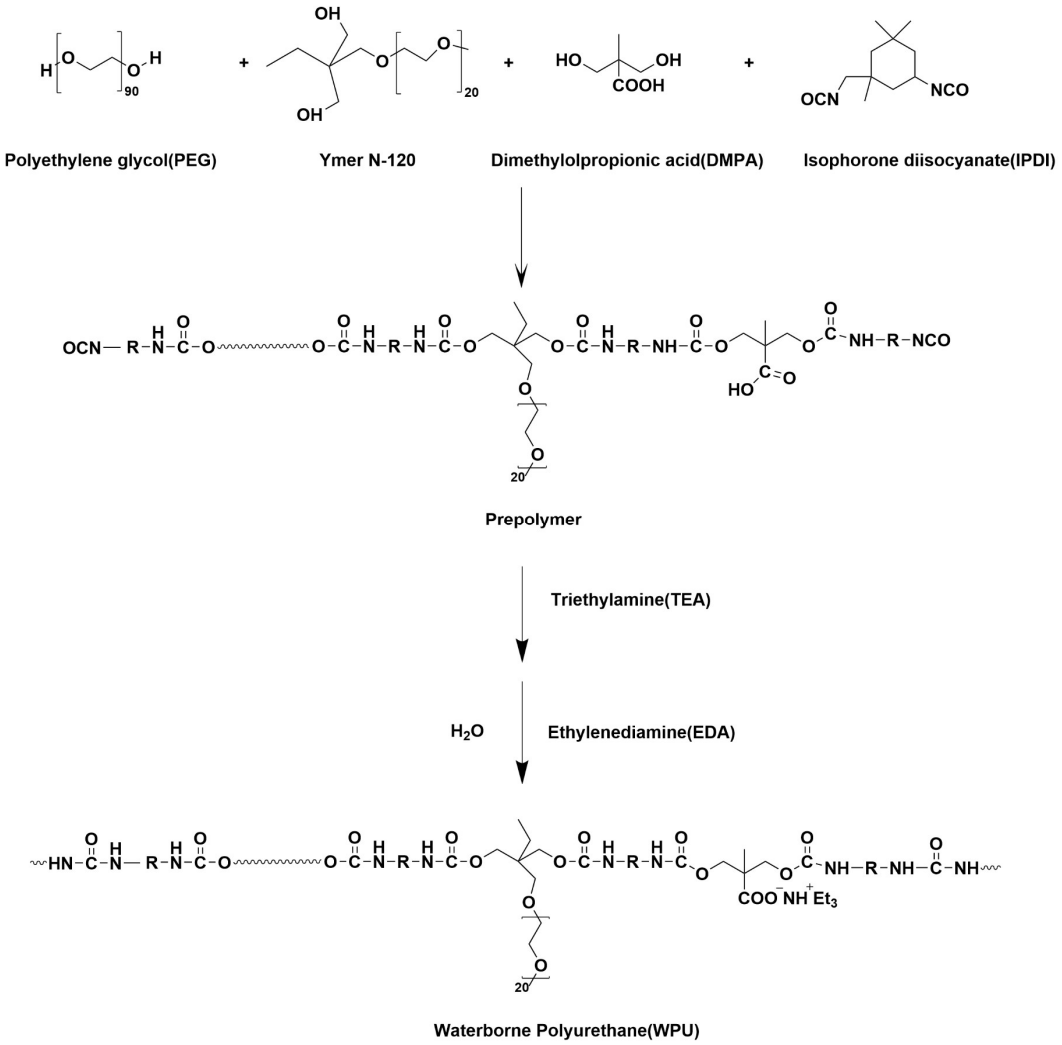

Fig. S1. Synthetic route and the structural formula of WPU.

Fig. S2. Photograph of WPU solution.

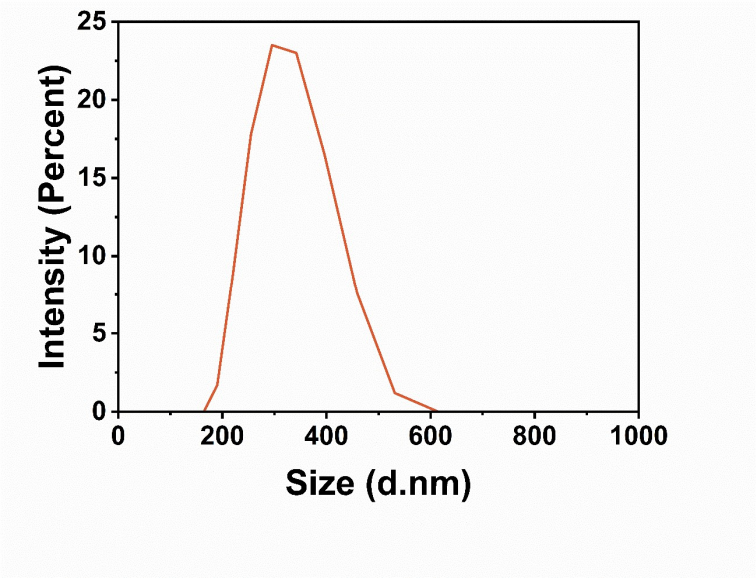

Fig. S3. The particle size distribution of WPU solution.

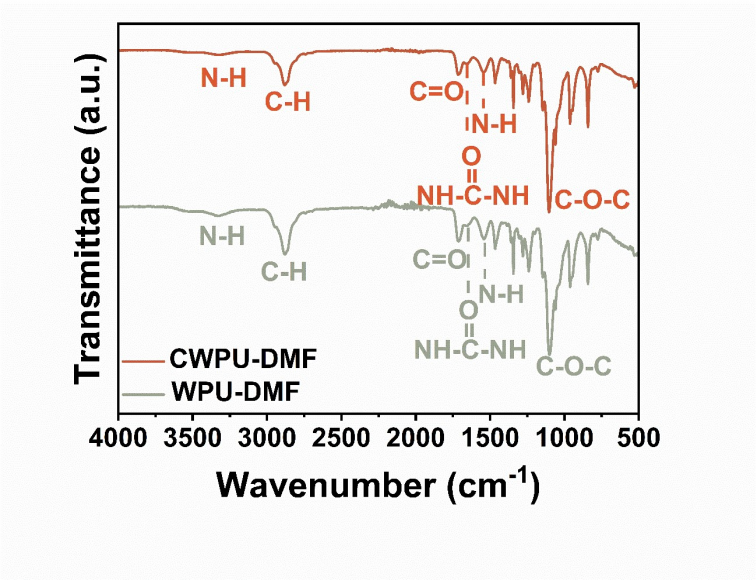

Fig. S4. FTIR spectra of dissolved WPU and CWPU polymers in DMF solution.

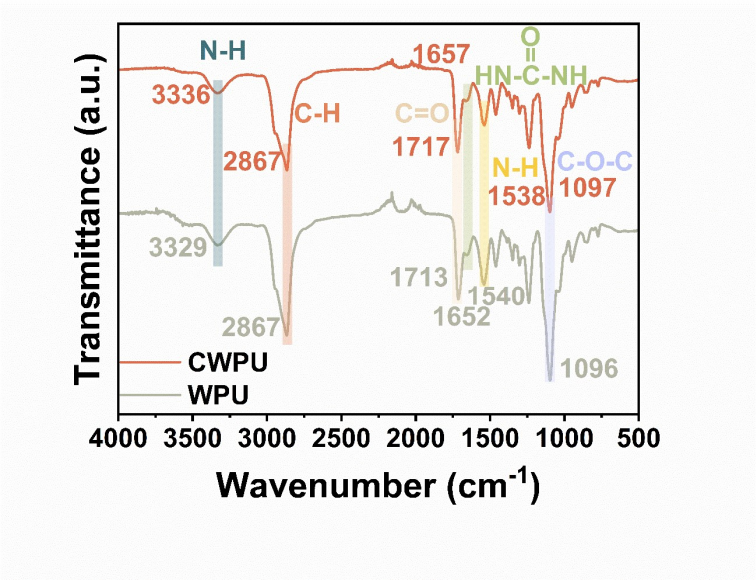

Fig. S5. FTIR spectra of CWPU and WPU.

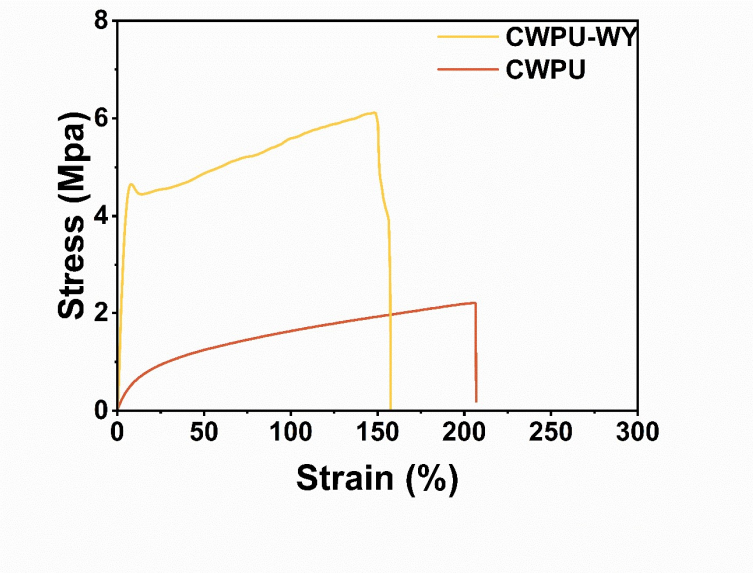

Fig. S6. The tensile stress-strain curves of CWPU and CWPU-WY.

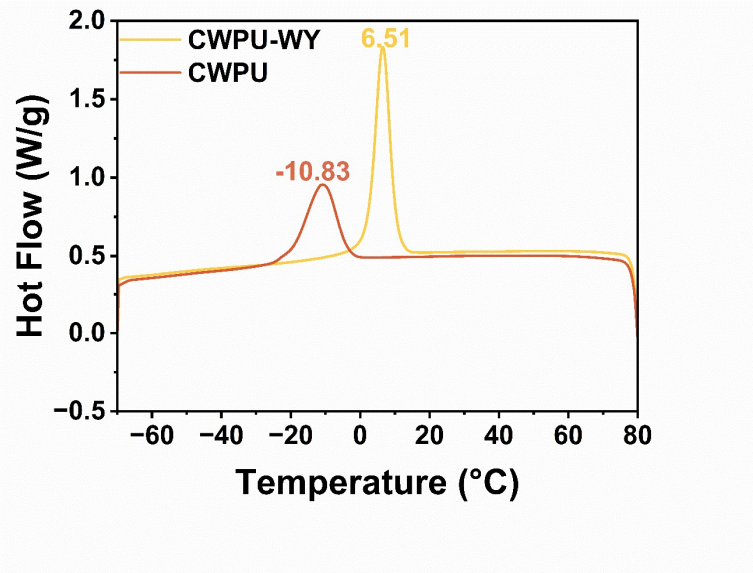

Fig. S7. The DSC curves of CWPU and CWPU-WY.

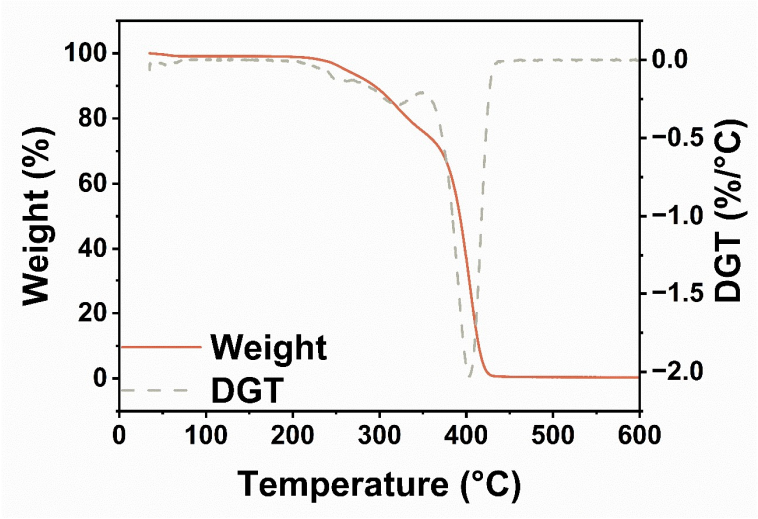

Fig. S8. The TGA curve of CWPU binder.

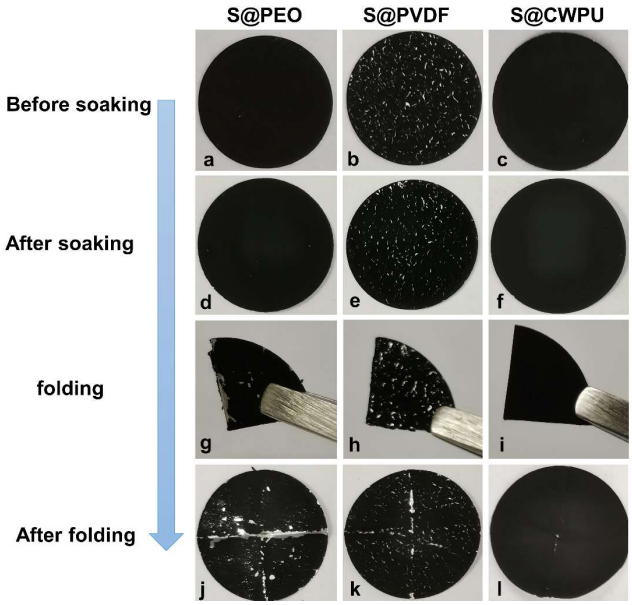

Fig. S9. The morphology of electrodes with PEO, PVDF, and CWPU binders (a-c) before and (d-e) after being soaked in electrolyte for 12 h. (g-i) The photos of folded electrodes with different binders after being soaked in electrolyte. (j-l) The electrodes were unfolded.

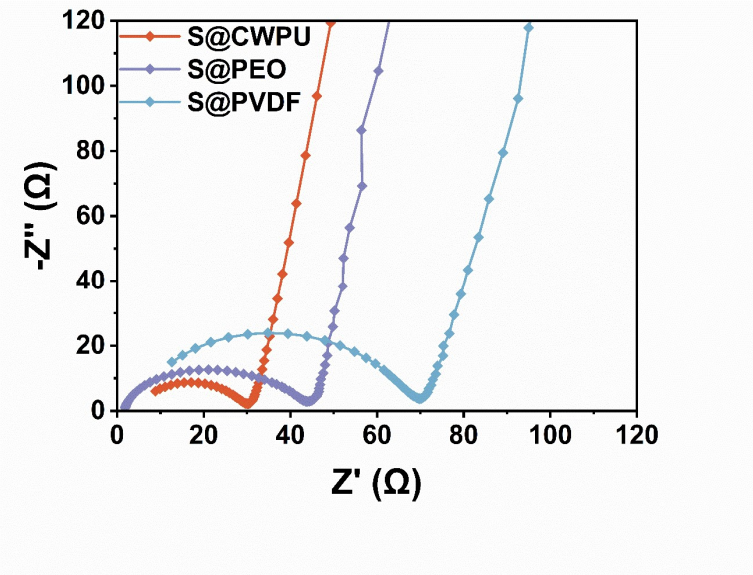

Fig. S10. The Nyquist plots of S@CWPU, S@PEO, and S@PVDF.

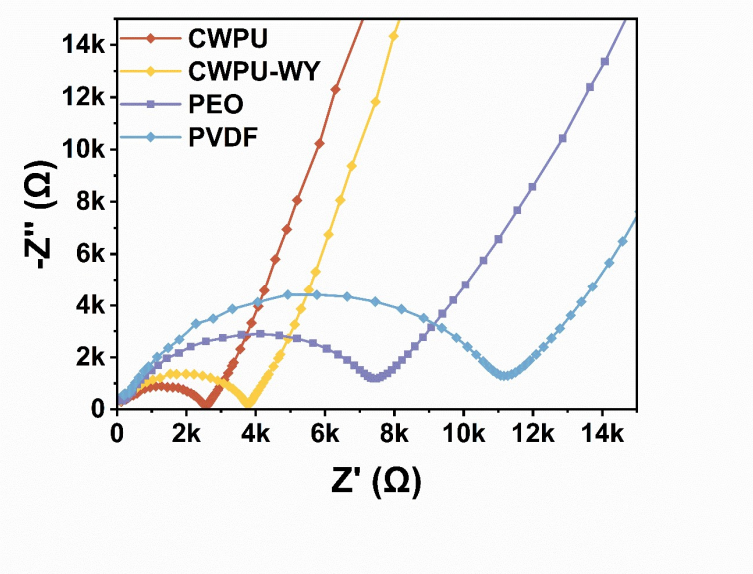

Fig. S11. The Nyquist plots of symmetric stainless-steel|binder membrane with LiTFSI| stainless-steel cell.

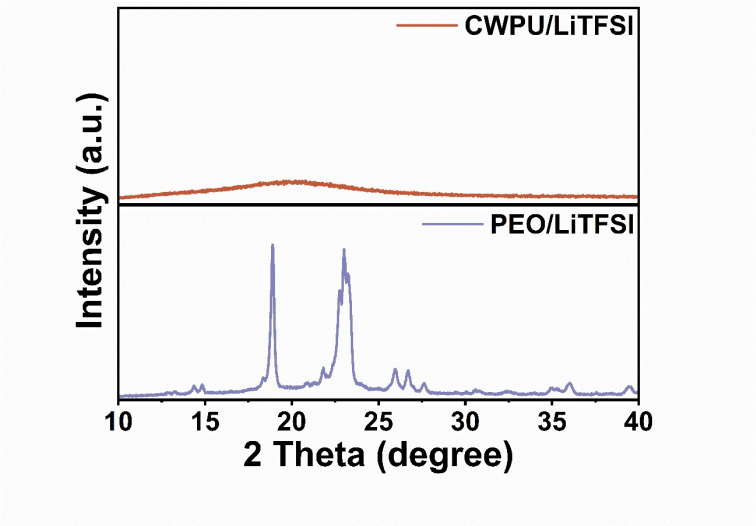

Fig. S12. XRD patterns of CWPU/ LiTFSI and PEO/ LiTFSI films.

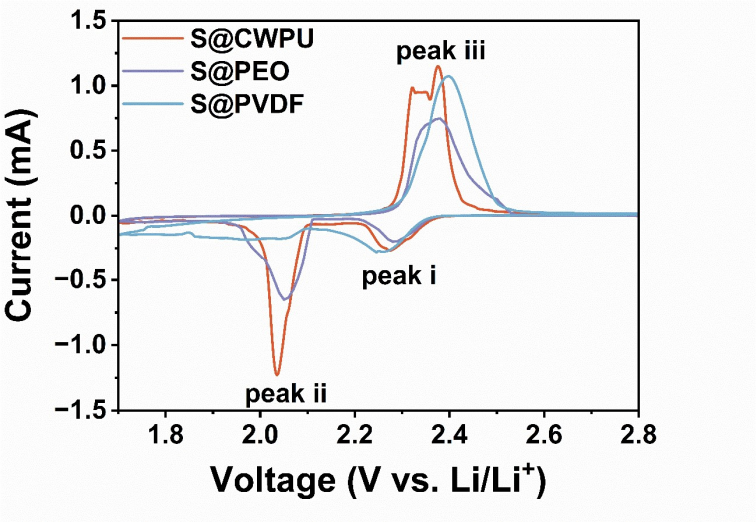

Fig. S13. The CV curves of batteries based on CWPU, PEO and PVDF binders at a scan rate of 0.033 mv s^{-1}.

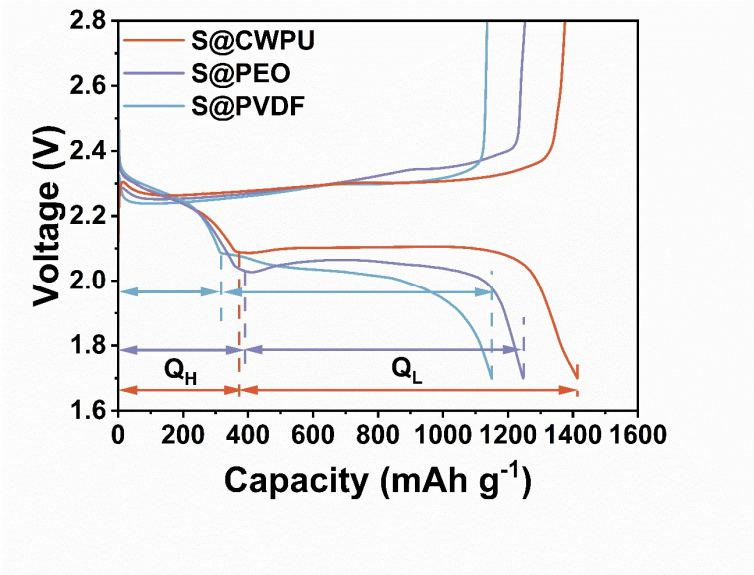

Fig. S14. The galvanostatic charge-discharge curves for the first cycle of the batteries with different binders at 0.1C.

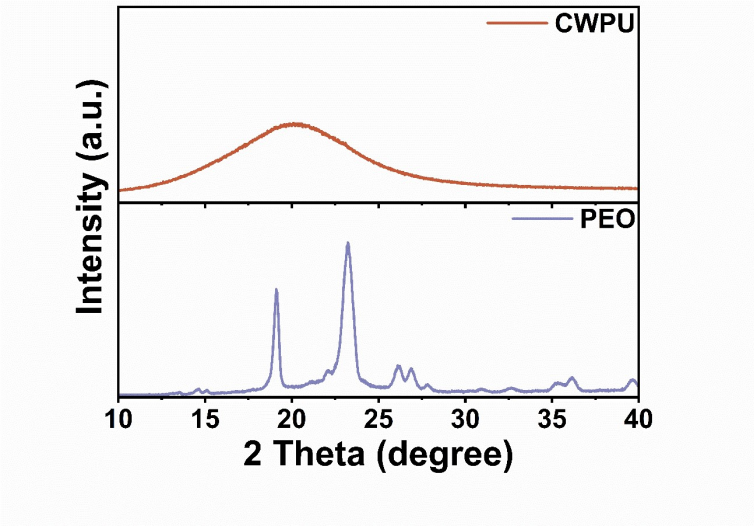

Fig. S15. XRD patterns of CWPU and PEO films.

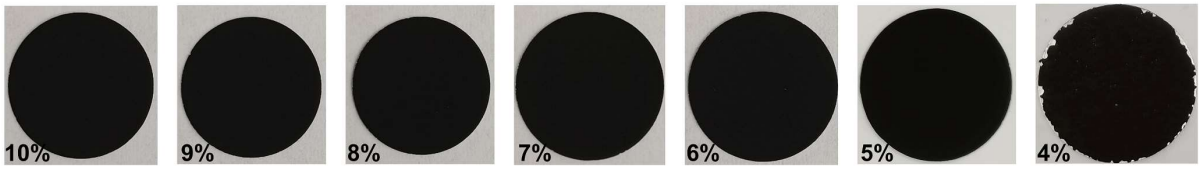

Fig. S16. The photographs depict electrodes with CWPU binder content ranging from 10% to 4%.

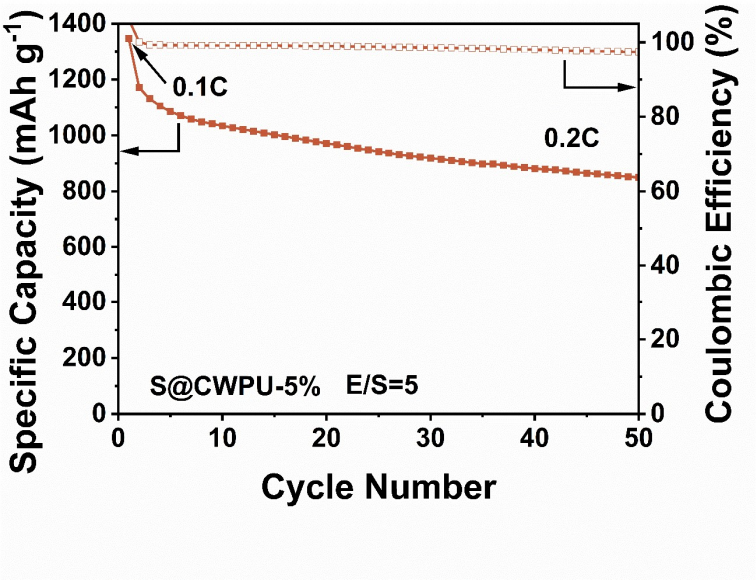

Fig. S17. The long-cycle performance of S@CWPU-5% under the condition of E/S=5.

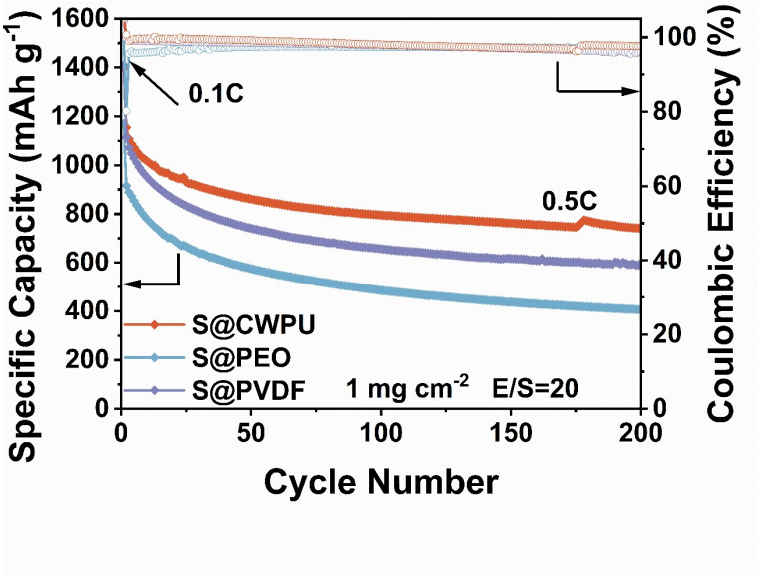

Fig. S18. The long-cycle performance of S@CWPU, S@PEO, and S@PVDF under the condition of E/S=20 (the ratio of electrolyte to sulfur is 20 μL mg^{-1}).

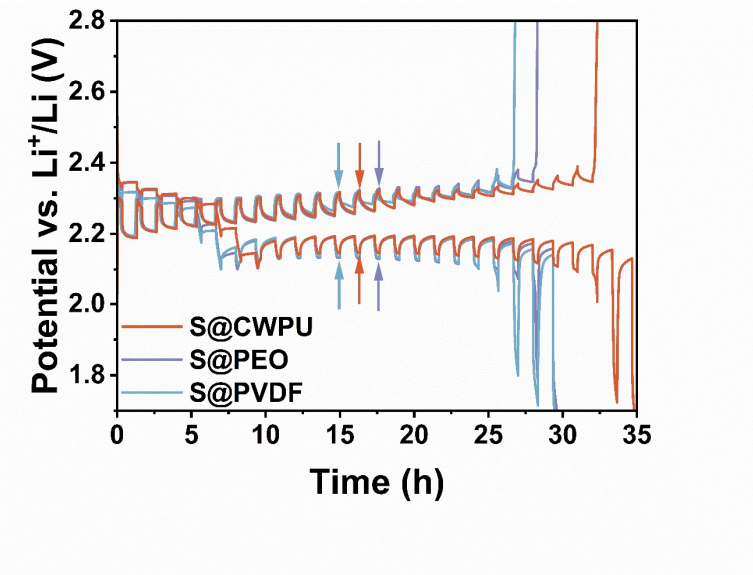

Fig. S19. The GITT curves of S@CWPU, S@PEO, and S@PVDF.

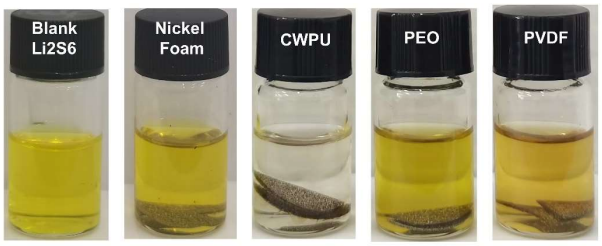

Fig. S20. Photographs of Li_2S_6-DME/DOL solutions after adsorbed with blank, nickel foam, CWPU, PEO and PVDF binders.

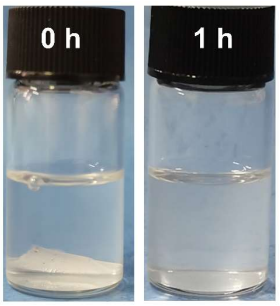

Fig. S21. Photographs depicting PEO film before and after dissolution in the electrolyte.

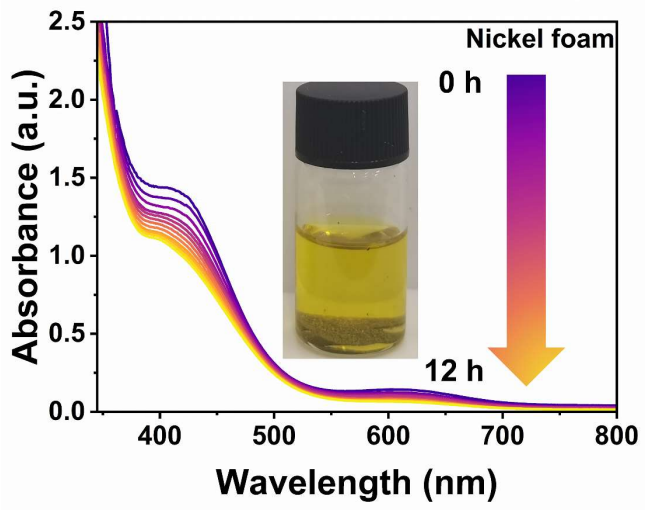

Fig. S22. UV-vis adsorption spectra of the Li_2S_6-DME/DOL solution with nickel foam.

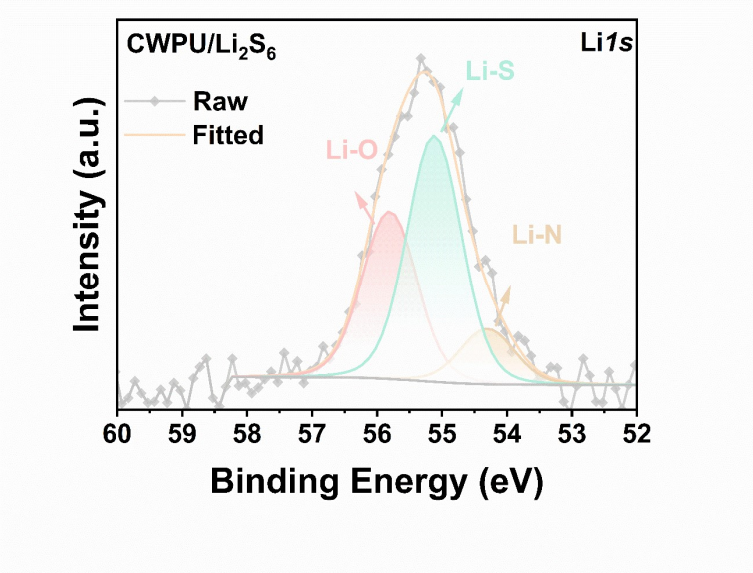

Fig. S23. The Li 1*s* peak of CWPU/Li_2S_6.

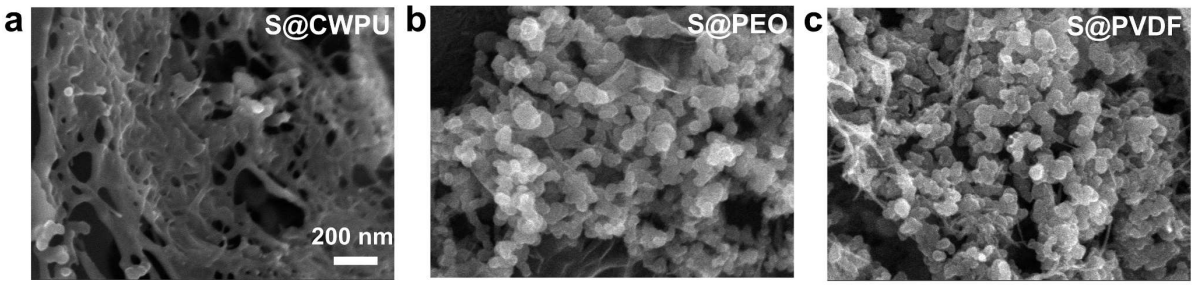

Fig. S24. The micromorphology observed by SEM of (d) S@CWPU, (e) S@PEO, and (f) S@PVDF before cycling.

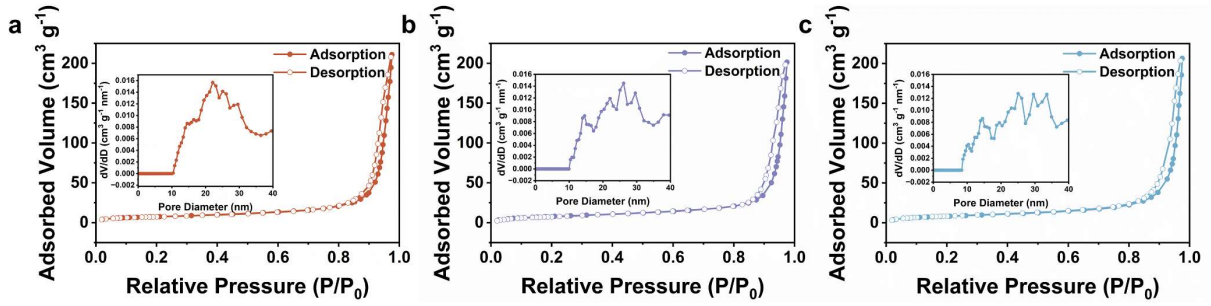

Fig. S25. The N_2 adsorption/desorption isotherms of CWPU, PEO and PVDF based electrodes, and the illustrations show the pore distribution.

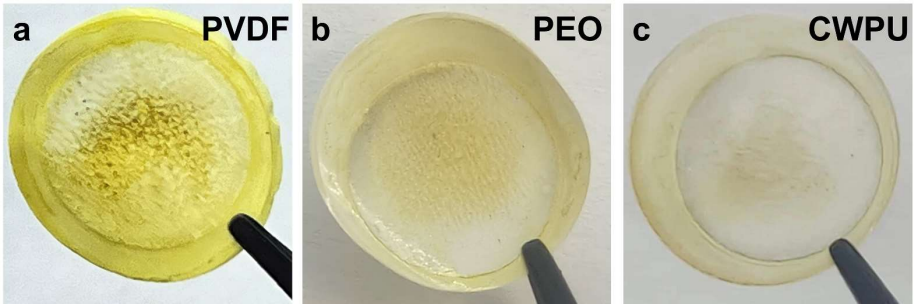

Fig. S26. Photographs of the separators from the batteries with (a) PVDF, (b) PEO, and (c) CWPU binders.

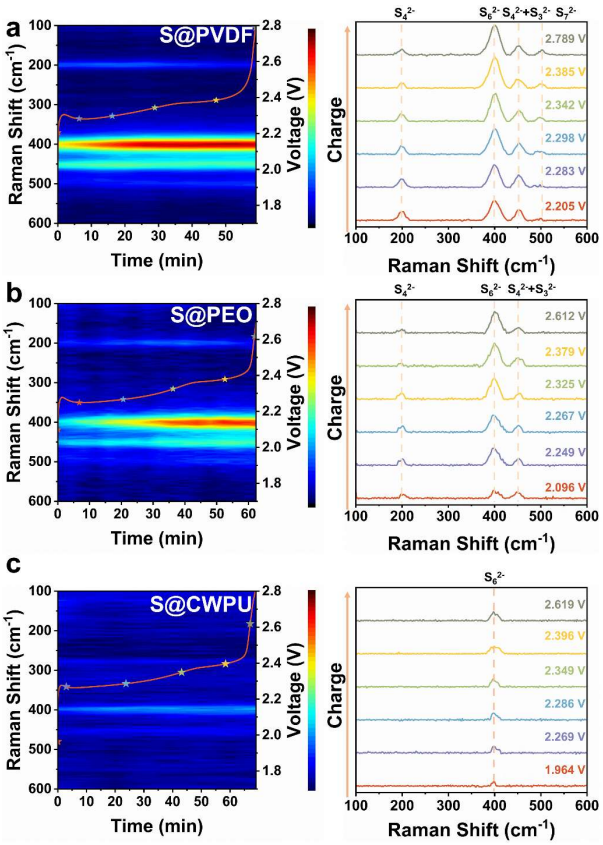

Fig. S27. The in-situ Raman spectra of (a) S@PVDF, (b) S@PEO, and (c) S@CWPU during the charging process at 0.5C.

3. Supplementary Tables

Table S1. The molar quantities of different materials to synthesis WPU and WPU-WY binders.

Material (mmol)	PEG	DMPA	Ymer N120	IPDI	TEA	EDA
WPU	4.50	7.68	6.30	25.88	7.68	7.40
WPU-WY	4.50	6.71	0.00	15.25	6.04	4.04

Table S2. The mass of the CWPU and WPU dissolved before and into DMF solution.

Sample	Before (g)	Dissolved in DMF (g)	Dissolved content
CWPU	0.285	0.041	14.4%
WPU	0.283	0.283	100%

Table S3. The Li-ion conductivity of CWPU, CWPU-WY, PEO, and PVDF binders.

Sample	L (cm)	A (cm^2)	$\sigma \times 10^{-5}$ ($S\ cm^{-1}$)
CWPU	0.0238	0.6400	1.4498
CWPU-WY	0.0241	0.6400	0.9963
PEO	0.0218	0.6400	0.4551
PVDF	0.0297	0.6400	0.4117

Reference

1 D. Gueon, M.-Y. Ju and J. H. Moon, *Proc. Natl. Acad. Sci.*, 2020, **117**, 12686–12692.

2 S. Yao, H. Yu, M. Bi, C. Zhang, T. Zhang, X. Zhang, H. Liu, X. Shen and J. Xiang, *Int. J. Energy Res.*, 2022, **46**, 19585–19598.

3 B. Jin, L. Yang, J. Zhang, Y. Cai, J. Zhu, J. Lu, Y. Hou, Q. He, H. Xing, X. Zhan, F. Chen and Q. Zhang, *Adv. Energy Mater.*, 2019, **9**, 1902938.

4 H. Wang, P. Zheng, H. Yi, Y. Wang, Z. Yang, Z. Lei, Y. Chen, Y. Deng, C. Wang and Y. Yang, *Macromolecules*, 2020, **53**, 8539–8547.